

## 2D Wavelet Transform on Extraction of Heartbeat Signal with Ultra-Wideband Impulse Radar

Khoa Nguyen Dang<sup>1\*</sup>, Tran Thi Van<sup>2</sup>, Pham Hai Yen<sup>1</sup>, Bui Thanh Tung<sup>1</sup>, Van Su Luong<sup>3</sup>, Minhhuy Le<sup>3</sup>

Submitted: 02/12/2023 Revised: 10/01/2024 Accepted: 26/01/2024

**Abstract:** Remote measurement of heartbeat signal is an essential task for health monitoring in smart hospital, smart home or smart car. Ultra-wideband impulse (UWB) radar is a potential device for accurate measurement of the heartbeat signal via remote distance. UWB radar allows measuring the heartbeat signal based on the tiny motion of the human thorax. However, the signal from the UWB radar includes not only the heartbeat signal but also interferences from noise and strong signal of the respiration. In this paper, we propose a method to improve of the signal-to-noise ratio (SNR) of the heartbeat signal based on two-dimension continuous wavelet transform (2DCWT). We performed experiments at different orientations and distances, and the results show that the 2DCWT method could efficiently extract the heartbeat signal with a root-mean-square error (RMSE) of 1.071 beats/min compared to a commercial photoplethysmography contact sensor. The proposed method could improve the SNR by about 17 dB on average compared to the 1D wavelet transforms filter method

**Keywords:** 2D wavelet transform, Heartbeat signal, Remote sensing, UWB radar

### 1. Introduction

Ultra-wideband impulse (UWB) radar for indoor applications consumes low power ( $< -41.3$  dBm) and wide bandwidth ( $> 0.5$  GHz). It is used in applications such as human tracking [1-3], human detection [4, 5], fall detection [6, 7], remote control [8], and health care [9, 10]. Among them, healthcare has been recently getting significant interest from both researchers and developers. Especially, the heartbeat signal measurement is for patient monitoring in the smart hospital, smart home, and smart car [9, 11, 12].

UWB radar could measure vital signals within a few meters by the small motion of thorax during the breathing and cardiac activities. The received signal of the UWB radar has two components which are stationary and non-stationary signals. The stationary signal is produced by static objects such as chairs, walls, furniture, etc. in the environment. The stationary signal could be simply removed by the mean subtraction or the singular value decomposition (SVD) method [13]. And, the non-stationary signals such as the respiration and heartbeat signals which produced by the motion of thorax during the breathing and cardiac activities. The heartbeat signal is usually very weak compared to the respiration signal and is easily buried in the noise signal. Therefore, the extraction of the heartbeat signal is a difficult task.

Numerous methods have been developed to enhance the heartbeat signal [14-22]. A higher-order cumulant (HOC) model

has been applied to improve the signal-to-noise ratio (SNR) of the heartbeat signal compared to the respiration signal by reducing the harmonics of the respiration signal; thus, it helps to determine the heartbeat frequency [14] more accurately. Harmonic path (HAPA) [15] and spectrum-averaged harmonic path (SHAPA) [16] algorithms have been developed for accurate detection of the heart rate. The HAPA and SHAPA use the harmonic components of the heartbeat signal to search the actual heart rate from the multiple noisy peaks. Continuous wavelet transform (1DCWT) was used to efficiently remove the noise from the heartbeat signal by the decomposition and composition of the signal [17, 18]. Higher harmonic components of the heartbeat signal were used to extract the heart rate [19]; the second or third harmonic components were used to minimize the effect of the harmonic components of the respiration signal. Accurate extraction of the heartbeat signal could be obtained by the extraction of eigenvalues of the vital signal [20-22]; two neighbor eigenvalues were used to reconstruct the heartbeat signal. These algorithms provide high accuracy of heartbeat signal extraction. However, those algorithms were applied to a univariate vital signal extracted at a single distance index of the person's position. If there was an error in the distance index selection or a large noise influence, the heartbeat signal could be inaccurately extracted.

In this paper, we propose a two-dimension continuous wavelet transform (2DCWT) for the extraction of the heartbeat signal. The 2D matrix of the vital signal in a range around the position of the person was used. The 2D signal processing was motivated by an observation that the vital signal of a person appears in a wide range distance according to the radar cross-section (RCS) and the heartbeat signals at distances have a correlation. Thus, the heartbeat signal could be accurately obtained by taking the correlation of the vital multivariate signal at different distances. In the 2DCWT algorithm, the 2D vital signal matrix is transformed in the two dimensions of the slow- and fast times

<sup>1</sup> Faculty of Applied Sciences, International School, Vietnam National University, Hanoi, Vietnam

ORCID ID : 0000-0002-6525-5245

<sup>2</sup> Faculty of General Education, University of Labour and Social Affairs, Hanoi, Vietnam

ORCID ID : 0000-0002-3351-4994

<sup>3</sup> Faculty of EEE, Phenikaa University, Hanoi 12116, Vietnam

ORCID ID : 0000-0001-6152-6215

\* Corresponding Author Email: khoand@vnui.edu.vn

based on the fast Fourier transform (FFT). The result is then correlated with a conjugate of a 2D wavelet to produce multiple-resolution scales. A method based on the total power of the cross-correlation between the vital signal and 2D Morlet wavelet was proposed to accurately select the scale corresponding to the heartbeat signal. Then, the heartbeat signal could be reconstructed at the selected scale by the inverse fast Fourier transform (IFFT). Finally, the heart rate was accurately obtained in the frequency domain by the Chirp-z transform (CZT).

## 2. Extraction of the heartbeat signal

### 2.1. Vital signal model

The measurement of vital signals by UWB radar is described in Fig. 1. The UWB radar measures the vital signal by the small motion of the thorax motion due to the breathing and cardiac motions. The motion of the thorax could be considered as a summation of the harmonic signals from the respiration activity and the cardiac activity. The displacement of the chest could be modeled as expressed in Eq. (1) [22]; where,  $d_{ri}$  and  $d_{hj}$  are the  $i$ -th and  $j$ -th harmonic displacement of the chest due to the respiration and cardiac activities respectively.  $f_r$  and  $f_h$  are fundamental of respiration and heart rates, respectively. And,  $t$  is the slow-time.

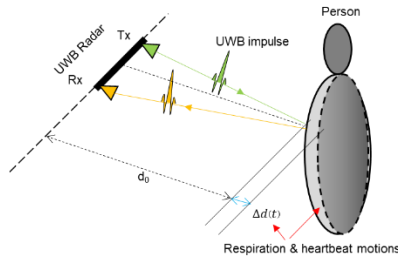


Fig. 1. Measurement model of the vital signal by UWB radar

$$\Delta d(t) = \sum_i d_{ri} \sin(2\pi f_{ri} t) + \sum_j d_{hj} \sin(2\pi f_{hj} t) \quad (1)$$

The received signal of the UWB radar is a summation of the signal reflected from the stationary objects and non-stationary objects, as expressed in Eq. (2), where  $A_k$  is the reflected coefficient of the object  $k$ -th,  $\tau_k$  is the fast-time delay of the object  $k$ -th, and  $P(\tau)$  is the collected pulses at the receiver. The first part of Eq. (2) is the signal from the stationary objects, the second part is the signal of the stationary part of the person's body, and the third part is the signal of the chest motion. The relationship between the fast-time and distance is expressed in Eq. (3), where  $c$  is the speed of light and  $N(\tau, t)$  is the random noise signal. The stationary objects such as chairs, walls, ceil, floors, and other furniture in the testing room produce DC signals. In the experiment, the person is sitting without moving; thus, the person's body is considered a stationary object except for the chest motion. The DC signals from the stationary objects could be removed by the mean subtraction [19, 21]. So, only the non-stationary signal (vital signal) and the random noise signal is remained, as expressed in Eq. (4). The vital signal  $X(\tau, t)$  contains the respiration signal, heartbeat signal, and noise signal.

$$X(\tau, t) = \sum_k A_k P(\tau - \tau_k) + A_0 P(\tau - \tau_0) + A_{\Delta d} P(\tau - \Delta\tau_0) + N(\tau, t) \quad (2)$$

$$\tau_k = 2d_k/c, \Delta\tau_0 = 2\Delta d(t)/c \quad (3)$$

$$X(\tau, t) = A_{\Delta d} P \left( \tau - \sum_i \frac{d_{ri}}{c} \sin(2\pi f_{ri} t) + \sum_j \frac{d_{hj}}{c} \sin(2\pi f_{hj} t) \right) + N(\tau, t) \quad (4)$$

$$X(\tau, t) = \sum_{k=1}^{+\infty} A_{rk} \sin(2\pi k f_r t) + \sum_{l=1}^{+\infty} A_{hl} \sin(2\pi l f_h t) + N(\tau, t) \quad (5)$$

The radar signal could be approximated as a quasi-periodic form, as expressed in Eq. (5) [20]; where,  $A_{rk}$  and  $A_{hl}$  are the amplitude of the harmonic order  $k$ -th and  $l$ -th of the respiration and heartbeat signal, respectively.  $N(\tau, t)$  is the noise signal. The vital signal  $X(\tau, t)$  contains the respiration signal, heartbeat signal, and noise signal.

Fig. 2 shows a simulation of the vital signal with and without noise signal. The respiration ( $f_r$ ) and heartbeat ( $f_h$ ) frequencies are 0.2 Hz and 1.3 Hz, respectively, and there are 2 harmonic components of the respiration signal ( $2f_r$ ,  $3f_r$ ). The heartbeat signal has much lower intensive than the respiration signal (1:10) due to small motion of in the heartbeat activity than the breathing activity. Thus, when the noise signal increase (-3dB, -10dB), the heartbeat signal is difficult to be detected. However, there is correlation pattern in the frequency domain among the distances, as observed in the bottom graphs of Fig. 2. Thus, it is feasible to extract the heartbeat signal by the 2D vital signal over a range distance rather than at a single distance as used in the previous studies [19, 20, 21].

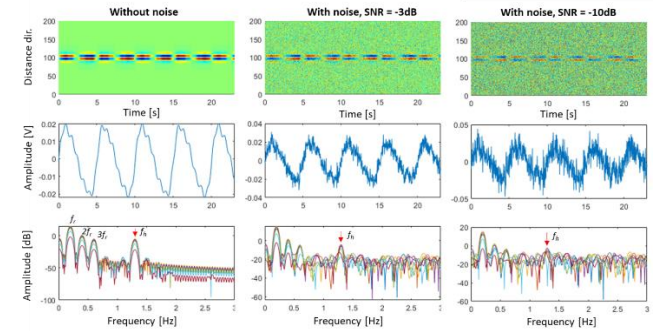
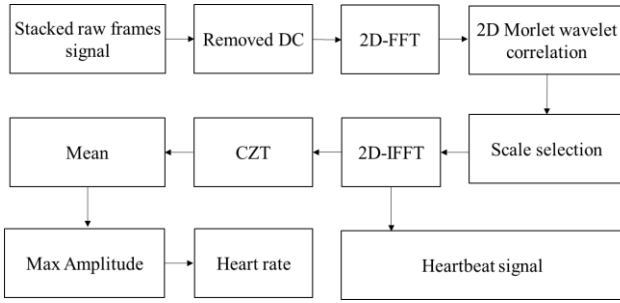


Fig. 2 Simulation of vital signal with noise and without noise. The heartbeat frequency ( $f_h$ ) is hard to be detected as the noise increase. But, correlation in frequency domain pattern appears among the distances that make it possible to detect the  $f_h$  via 2D signal analysis rather than at a single distance.

### 2.2. Continuous wavelet transform (2DCWT) algorithm

Fig. 3 shows the block diagram of the proposed algorithm for extracting the heartbeat signal by the 2DCWT. The received radar signal is stacked frame by frame to form a 2D matrix data  $X(i, j)$  with  $i = 1, 2, \dots, M$  and  $j = 1, 2, \dots, N$  representing for time index and distance index, respectively. The DC component in the received signal is removed by mean subtraction [19, 21]. To estimate the distance of a person, the power of the vital signal is used, as described in Eq. (6). The vital power is calculated through the square of the vital signal in the slow-time direction. The vital power in Fig. 4 shows that the person's distance could be estimated at the maximum power.

Furthermore, the high power of the vital signal that appears in a range around the person's position also be useful to extract the heartbeat signal. This range is called the radar cross-section (RCS). The RCS is depended on the radar bandwidth and object size. In this paper, with the bandwidth of 550 MHz, the RCS is average about 500 mm for adult people.



**Fig. 3** Block diagram of the heartbeat signal extraction by 2D Continuous wavelet transform

$$P(i) = \sum_{j=1}^N X^2(i, j) \quad (6)$$

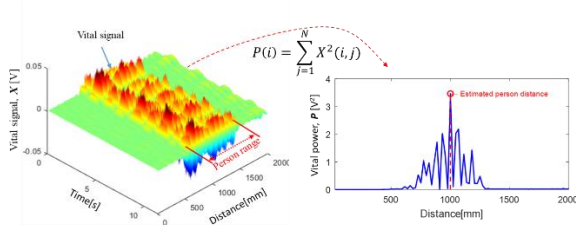


**Fig. 4** Vital signal appear around the person location which is determined by the vital power

CWT is an advanced signal analysis technique for non-stationary signals such as the heartbeat signal [21, 23]. In CWT, the length of the window is various at different frequency bands, which is more flexible and useful than a fixed window length in the short-time Fourier transform [23]. CWT could provide a good frequency resolution for a low-frequency signal and a good time resolution for a high-frequency signal. The 2D data of  $X(i, j)$  will be used in the 2DCWT of our proposed algorithm to extract the heartbeat signal. The 2DCWT algorithm has four steps as following:

*Step 1: 2D Fast Fourier transform signal (FFT)*

The FFT is performed on the 2D vital signal  $X$  as expressed in Eq. (7) [24, 25]; where  $p = 1, 2, \dots, M$ ,  $q = 1, 2, \dots, N$ , and  $i$  denotes the imaginary unit.

$$Y(p, q) = \sum_{i=1}^M \sum_{j=1}^N e^{-\frac{2\pi i(i-1)(p-1)}{M}} e^{-\frac{2\pi i(j-1)(q-1)}{N}} X(i, j) \quad (7)$$

*Step 2: 2D wavelet correlation*

A 2D mother Morlet wavelet  $W$  is shifted and scaled before taking cross-correlation with the FFT signal  $Y$ . The Fourier transform of the 2D mother Morlet wavelet is described by Eq. (8) [26, 27]; where,  $S$  is the integer scale vector, and  $\sigma$ ,  $w_0$  and  $\epsilon$  are the constant value. The  $w_x$  and  $w_y$  are shifts which are the functions of the  $M$ ,  $N$  and  $S$  as described in Eqs. (9) and (10). It is noted that the  $\mathbb{Z}(x)$  is the integer of  $x$ . A sample of a 2D

mother Morlet wavelet is shown in Fig. 5.

$$W(S, w_x, w_y) = S e^{-\sigma^2[(w_x - w_0)^2 + (\epsilon w_y)^2]} \quad (8)$$

$$w_x \quad (9)$$

$$= S \frac{2\pi}{N} \begin{bmatrix} 0 & 1 & \dots & \mathbb{Z}\left(\frac{N-1}{2}\right) & -\left[\mathbb{Z}\left(\frac{N-1}{2}\right) + 1\right] & \dots & 0 & -1 \\ \dots & \dots & \dots & \dots & \dots & \dots & \dots & \dots \\ 0 & 1 & \dots & \mathbb{Z}\left(\frac{N-1}{2}\right) & -\left[\mathbb{Z}\left(\frac{N-1}{2}\right) + 1\right] & \dots & 0 & -1 \end{bmatrix}_{M \times N}$$

$$w_y = S \frac{2\pi}{M} \begin{bmatrix} 0 & \dots & 0 \\ 1 & \dots & 1 \\ \dots & \dots & \dots \\ \mathbb{Z}\left(\frac{M-1}{2}\right) & \dots & \mathbb{Z}\left(\frac{M-1}{2}\right) \\ -\left[\mathbb{Z}\left(\frac{M-1}{2}\right) + 1\right] & \dots & -\left[\mathbb{Z}\left(\frac{M-1}{2}\right) + 1\right] \\ \dots & \dots & \dots \\ 0 & \dots & 0 \\ -1 & \dots & -1 \end{bmatrix}_{M \times N} \quad (10)$$

The relationship between the frequency ( $f$ ) and the scales ( $S$ ) for Morlet wavelet could be estimated as Eq. (11), where  $f_c$  is the center frequency of the 1D Morlet wavelet (0.8125 Hz), which is expressed in Eq. (12), and  $\Delta T$  is the frame sampling period [28]. Fig. 7(b) shows the relationship between the frequency ( $f$ ) and the scales ( $S$ ). It is clear that the heartbeat frequency in the range of 0.75 Hz to 3.0 Hz corresponds to the scales from 48 down to 12.

$$f = \frac{f_c}{S \Delta T} \quad (11)$$

$$\psi(t) = e^{-\frac{t^2}{2}} \cos(5t) \quad (12)$$

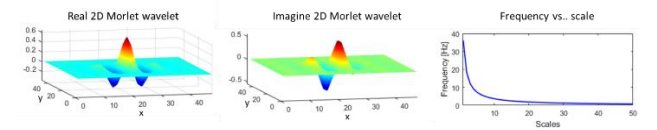


**Fig. 5** The real (a) and imagine (b) 2D Morlet wavelet and the relationship between the scale  $s$  and frequency  $f(c)$

The cross-correlation between the vital signal and 2D Morlet wavelet is expressed in term  $F$ , as described in Eq. (13), where  $*$  denotes the complex conjugate. The cross-correlation is a complex 3D matrix with a size of  $M \times N \times N_s$ , where  $N_s$  is the length of the scale vector  $S$ .

$$F(s, p, q) = Y(p, q) \cdot W(s, w_x, w_y)^* \quad (13)$$

*Step 3: Scale selection and reconstruction of vital signal*

Correct identification of the scale corresponding to the heart rate is the most important task of the algorithm. In this step, we use the total power of the  $F$  in each scale to search the correct scale of the heartbeat signal. The total power of  $F$  in the  $s$ -th scale ( $D(s)$ ) is expressed in Eq. (14). And, the maximum peak of the total power corresponds to the heartbeat signal. Fig. 6 shows an example of the  $D$  with the scales  $s$  and time index  $q$ . There is an interference of the harmonic of the respiration signal in the power  $D$  since the power of the harmonic signal is higher than the power of heartbeat signal. However, the heartbeat signal forms a peak in the spectrum. Thus, the correct scale could be determined at the peak power (for instance,  $s_{peak} = 25$  for the example data in Fig. 6). Then, the heartbeat signal  $\hat{X}$  could be reconstructed by the inverse FFT (iFFT) of the  $F(s_{peak})$ , as

expressed in Eq. (15) [29].

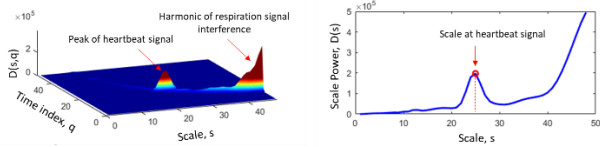


**Fig. 6** Selection of scale for the heartbeat signal

$$D(s) = \sum_{p=1}^M \sum_{q=1}^N F(s, p, q)^2 \quad (14)$$

For  $s = 1, 2, \dots, Ns$

$$\hat{X}(i, j) = \frac{1}{MN} \sum_{p=1}^M \sum_{q=1}^N e^{\frac{2\pi i(p-1)(i-1)}{M}} e^{\frac{2\pi i(q-1)(i-1)}{N}} F(s_{peak}, p, q) \quad (15)$$

For  $i = 1, 2, \dots, M$  and  $j = 1, 2, \dots, N$

#### Step 4: Heart rate extraction

The final step is the extraction of the heart rate from the reconstructed signal  $\hat{X}$ . The signal is then converted to the frequency domain by using the CZT in the range from 0.0 to 3.0 Hz. The upper limit of 3.0Hz is set same as the maximum range of the heart rate of a normal person [21, 22], and there is no lower limit (0 Hz) to see whether the respiration signal remains in the heartbeat signal. The signal in the frequency domain is then averaged ( $\hat{C}$ ), as expressed in Eq. (16) and the maximum peak indicates the heart rate.

$$\hat{C}(j) = \frac{1}{M} \sum_{i=1}^M C(i, j) \quad \text{where } C(i, j) \text{ is the CZT of } \hat{X}(i, j) \quad (16)$$

## 3. Experimental results

### 3.1. Experimental setup

A UWB radar (UWB-Radar 4.6, UMAIN Inc. Korea) was used in the experiment to demonstrate our proposed method, as shown in Fig. 7. The UWB radar has 4.6 GHz center frequency, 550MHz bandwidth, and less than -41.3dBm output power. The radar was supplied by 5V and signal transmission via a USB cable to a computer. The beam angle of the transmitter and receiver antennas is about 75-80 degrees. The distance sampling resolution is 20.3 cm. The maximum range of measurement is about 13 m that corresponds to the 660 distance samples in a single frame. The frame rate of the signal transmitted from the radar to the computer is about 44.5 frames/s via UART protocol. The detailed specifications of the UWB radar are shown in Table 1.

**Table 1** Specification of the UWB radar

Parameters	Specification
Center frequency	4.6 GHz
Bandwidth	550 MHz
Distance resolution	20.3 cm
Antenna's type	Directional
Antennas beam angle in X-Z Plane	75°
Antennas beam angle in Y-Z Plane	80°
Voltage supply	5V via USB cable
Max current consumption	350 mA
Output power	< -41.3 dBm

Radar frame rate

44.5 frames/s

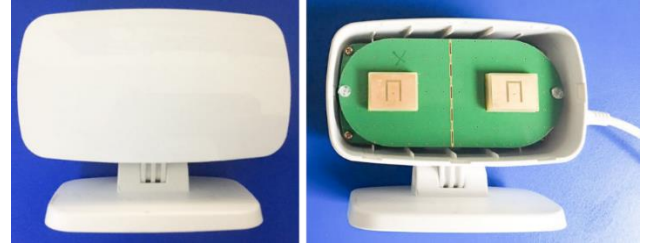


**Fig. 7** UWB radar used in the experiment

The experimental scenario is shown in Fig. 8. The UWB radar was placed to a person with a distance from 0.5 to 2.0 m. An adult person sits on the chair and breathing normally at four orientations, which are 0-degree (front), 45-degree, 90-degree (lateral), and 180-degree (backside). During the experiment, a photoplethysmography (PPG, Ubpulse 360) sensor is used to measure the heartbeat signal at a finger as the reference. The vital signal was measured simultaneously by both the UWB radar and PPG sensors. All sensors are connected to the desktop PC via a USB connection for power supplies and data acquisition.

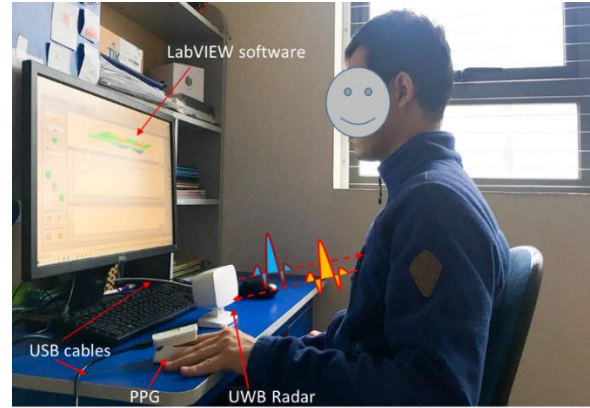


**Fig. 8** The UWB radar configuration system

### 3.2. Heartbeat signal extraction

In this section, we show some results in different experimental scenarios. The distances between the person and UWB radar are 0.5m, 1.0m, and 2.0m, and the orientation of the person is rotated with 0-degree (front side), 45-degree, 90-degree (lateral side), and 180-degree (backside). The 2D matrix of the vital signal ( $X$ ) was stacked with 512 frames ( $N = 512$ ) signal. The proposed 2DCWT method was compared with the 1D continuous wavelet transform [30] (denoted as 1DCWT) method and the PPG referenced signal. For quantitative comparison, the SNR is calculated as described in Eq. (17) [32].

$$SNR = 20 \log \frac{\sum C_{Heartbeat}}{\sum C_{Respiration} + \sum C_{Noise}} \quad (17)$$

Fig. 9 shows the raw vital signal, and processed signal of 1DCWT, 2DCWT-Full scale, and 2DCWT-Peak scale methods for an experiment at the distance of 1.0 m and the front side orientation. Similar to the results in Fig. 6, the respiration signal is the dominant signal that could be observed in the frequency



domain of the raw vital signal (Fig. 9a). In addition, the second harmonic of the respiration signal (0.74 Hz) was even higher than the fundamental of the heartbeat signal (1.494 Hz). Therefore, the 1DCWT method was failed to extract the correct the heartbeat frequency as the second harmonic of the respiration signal remained in the extraction result; thus, the SNR was low (-9.0 dB). Similarly, the 2DCWT-Full scale also extracted this harmonic signal and enhanced it only (the largest one) while decreasing the heartbeat signal (SNR = -17.7 dB). So, the 1DCWT and 2DCWT-Full scale were provided the wrong detection of the heart rate. However, the 2DCWT-Peak scale was significantly enhanced the heartbeat signal (SNR = 6.3 dB) because of the correct selection of the scale (speak = 29). And, the heartbeat frequency extracted from the 2DCWT-Peak scale method was 1.488 Hz which is only one resolution tolerance (0.4%) from the referenced PPG signal (1.494 Hz).

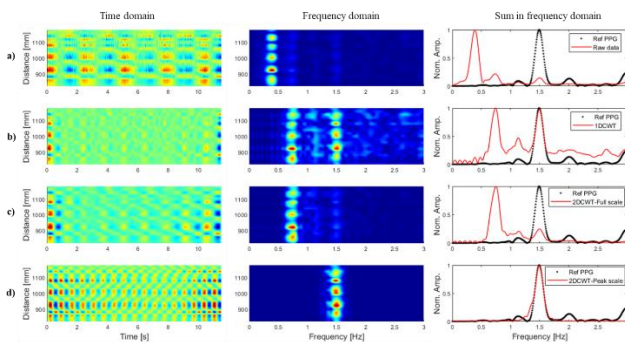


**Fig. 9** Extraction of the heartbeat signal at the distance of 1.0 m – front side orientation: a) raw, vital signal, b) 1DCWT method, c) 2DCWT-Full scale method, and d) 2DCWT-Peak scale.

Similarly, and the results of the backside orientation are shown in Fig. 10. The 2DCWT-Peak scale correctly extracted the heartbeat signal with a significant enhancement (SNR = 4.6 dB) while the 1DCWT enhanced both the second harmonic of the respiration signal and the fundamental of the heartbeat signal, and the 2DCWT-Full scale only enhanced the second harmonic of the respiration signal. Thus, the 1DCWT and 2DCWT-Full scale provided low SNR which are, -26.4 dB and -24.1 dB, respectively. The extraction of the heart rate by the 2DCWT-Peak scale method was 1.553 Hz, slightly different with the PPG reference (1.565 Hz, 0.7%). In addition, it is observed in the frequency domain that more noise signal appeared in the backside orientation than in the front side orientation due to extra noise signal as the electromagnetic wave propagates through the person body to the chest (the chest is opposite to the UWB radar). However, the 2DCWT-Peak scale method still correctly detected the heartbeat signal.

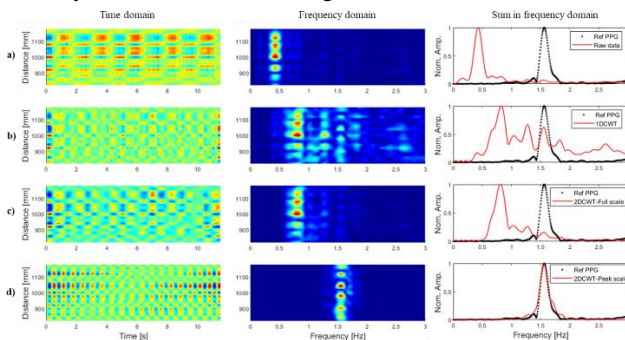


**Fig. 10** Extraction of the heartbeat signal at the distance of 1.0

m – backside orientation: a) raw vital signal, b) 1DCWT method, c) 2DCWT-Full scale method, and d) 2DCWT-Peak scale method.

More results in the frequency domain of the heartbeat signal at different distances and orientations are shown in Fig. 11. The results show that the 2DCWT-Peak scale method could help improve the SNR of the heartbeat signal while the 1DCWT and 2DCWT-Full scale methods still retain the second harmonic of the respiration signal. The detailed SNRs of the heartbeat signal are shown in Table 2. The 2DCWT-Peak scale method could improve the SNR of the heartbeat signal with an average of 53.8dB, better than the 1DCWT and 2DCWT-Full scale methods with 20.0dB and 25.3dB (compare to the raw signal), respectively. The main reason why the 2DCWT-Full scale method provides the worst improvement is because it was influenced by the high intensity of the second harmonic of the respiration signal.

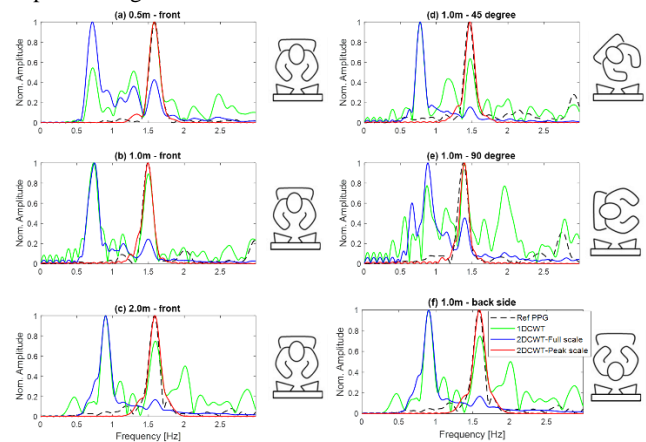


**Fig. 11** Frequency domain of the heartbeat signal at different distances and orientations of the person

**Table 2** SNR of the heartbeat signal at different distances and orientations [unit: dB]

Orientation distance	Raw signal	1DCWT	2DCWT-Full scale	2DCWT-Peak scale
Front - 0.5m	-49.6	-9.3	-15.7	8.4
Front - 1.0m	-46.4	-9.0	-17.7	6.3
Front - 2.0m	-49.1	-13.6	-21.6	5.1
45 deg-1.0m	-45.7	-11.8	-19.7	6.6
Lateral-1.0m	-45.0	-11.7	-15.3	7.0
Back - 1.0m	-49.0	-26.4	-24.1	4.6

### 3.3. Heart rate monitoring

Heart rate monitoring is an important task of heartbeat measurement system. The full block diagram of the heartbeat signal monitoring based on the 2DCWT-Peak scale filter is shown in Fig. 12. The vital signal was stacked in a window with 512 frames corresponding to 11.4 s. window and shifted by 1 frame during the monitoring. The person range was automatically selected by the vital power, as described in Section 2. After extraction of the heartbeat signal by the proposed 2DCWT algorithm, the heartbeat signal is transformed in to the frequency domain by the CZT. To remove the noise that may occur during the monitoring, the exponential moving

average ( $\bar{C}$ ) is applied to smooth the CZT signal ( $\hat{C}$ ).  $\bar{C}$  is updated from the previous  $\bar{C}$  and the current input  $\hat{C}$ , as expressed in Eq. (18); where  $0 < \alpha < 1$  is the coefficient which is inversely proportional to the number of averaging frames ( $N_{avr}$ ) with  $\alpha = 2/(N_{avr} + 1)$ .

$$\bar{C} = \alpha \hat{C} + (1 - \alpha) \bar{C} \quad (18)$$

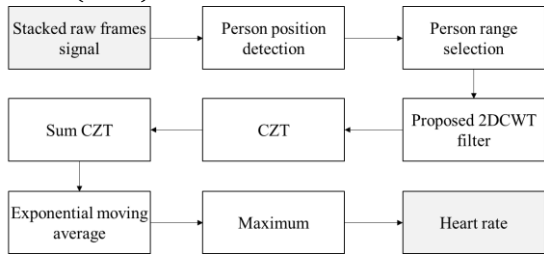


**Fig. 12** Block diagram of the heart rate monitoring by the 2DCWT-Peak scale algorithm

Fig. 13 shows the spectrogram of the heart rate monitoring results, including raw vital signal, 1DCWT method, 2DCWT-Full scale method, and the 2DCWT-Peak scale method. The heart rates in both the UWB radar and the reference PPG sensor are strongly disturbed while the person is moving into and out of the chair at the time [0s-5.5s] and [97s-100s], respectively. So, we only consider the stable state of the person while sitting on the chair. The spectrogram of the raw vital signal shows that the harmonics of the respiration signal can be observed clearly, which is much higher than the heartbeat signal. The 1DCWT method provides a mixing of the heartbeat signal and the second harmonic of the respiration signal in the spectrogram. The heart rate was not continuously monitored and was disturbed by the strong noise, such as in the time from 62s to 90s. The 2DCWT-Full scale method provides a better noise reduction result than the 1DCWT method, but the second harmonic of the respiration signal was significantly enhanced and dominated the heartbeat signal. The 2DCWT-Peak scale method provides the best result, which accurately extract the heart rate. Heart rate monitoring results are shown in Fig. 14. The root-mean-square error of the 1DCWT, 2DCWT-Full scale, and 2DCWT-Peak scale methods compared to the reference PPG sensor are 14.5 BPM, 19.0 BPM, and 1.1 BPM, respectively. The transient time for getting a stable value of the heart rate after the stable sitting of the 2DCWT-Peak scale method is about 9s.

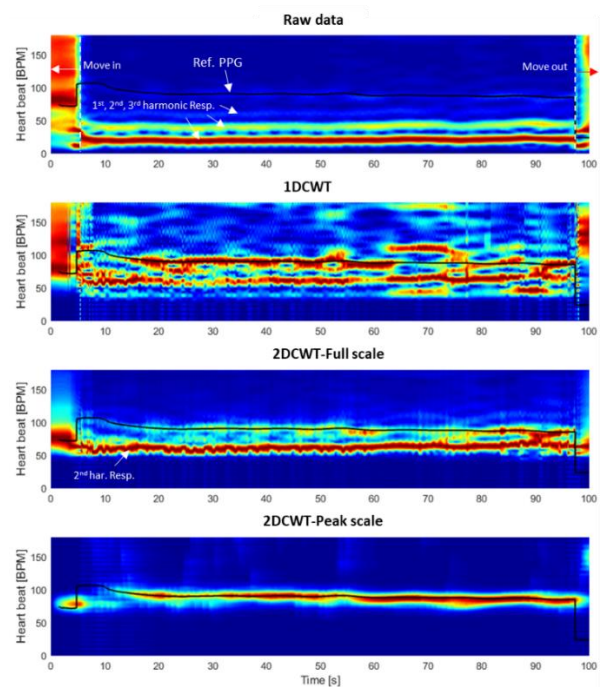


**Fig. 13** Spectrogram of the heartbeat monitoring

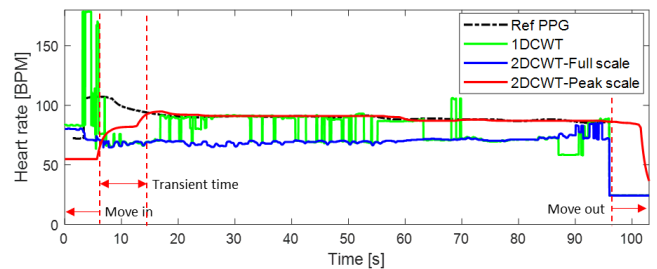


**Fig. 14** Heart rate monitoring results

## 4. Conclusions

This paper proposes a 2D continuous wavelet transform (2DCWT) method for the extraction of the heartbeat signal of a UWB radar. The 2D matrix of the vital signal is extracted from the raw signal of the UWB was used. The 2D input vital signal was transformed to the frequency domain by the 2D fast Fourier transform (2DFFT). Then, the cross-correlation between the 2DFFT and a 2D Morlet wavelet was taken by the scaling and shifting the 2D Morlet wavelet. The maximum peak in the total power of this correlation was found to be corresponding to the heartbeat signal. The time-domain vital signal was then reconstructed from the selected scale and the 2D invert FFT. The heart rate is then further found by the Chirp-z transform, which provides high-frequency resolution in a range of the normal heart rate. The proposed 2DCWT showed a good improvement of the SNR of the heartbeat signal and high accuracy of the heart rate.

## Acknowledgement

This research is funded by International School, Vietnam National University, Hanoi (VNU-IS) under project number CS.2023-02.

## References

- [1] H. Xue *et al.*, "An Algorithm Based Wavelet Entropy for Shadowing Effect of Human Detection Using Ultra-Wideband Bio-Radar," *Sensors*, vol. 17, no. 10, 2017.
- [2] S. Chang, R. Sharan, M. Wolf, N. Mitsumoto, and J. W. Burdick, "People Tracking with UWB Radar Using a Multiple-Hypothesis Tracking of Clusters (MHTC) Method," *International Journal of Social Robotics*, vol. 2, no. 1, pp. 3-18, 2010/03/01 2010.
- [3] S. Chang, M. Wolf, and J. W. Burdick, "Human detection and tracking via ultra-wideband (UWB) radar," in *IEEE International Conference on Robotics and Automation*, 2010, pp. 452-457: IEEE.
- [4] A. Yarovoy, L. Lighthart, J. Matuzas, and B. Levitas, "UWB radar for human being detection," *IEEE Aerospace Electronic Systems Magazine*, vol. 23, no. 5, pp. 36-40, 2008.
- [5] S. Chang, N. Mitsumoto, and J. W. Burdick, "An algorithm for UWB radar-based human detection," in *IEEE Radar Conference*, 2009, pp. 1-6: IEEE.
- [6] T. Han, W. Kang, and G. Choi, "IR-UWB Sensor Based Fall Detection Method Using CNN Algorithm," *Sensors*, vol. 20, no. 20, 2020.
- [7] L. Ma, M. Liu, N. Wang, L. Wang, Y. Yang, and H. Wang, "Room-Level Fall Detection Based on Ultra-Wideband (UWB) Monostatic Radar and Convolutional Long Short-Term Memory (LSTM)," *Sensors*, vol. 20, no. 4, 2020.
- [8] I. Immoreev and S. Ivashov, "Remote monitoring of human cardiorespiratory system parameters by radar and its applications," in *4th International Conference on Ultrawideband and Ultrashort Impulse Signals*, 2008, pp. 34-38: IEEE.
- [9] H.-S. Cho and Y.-J. Park, "Detection of heart rate through a wall using UWB impulse radar," *Journal of healthcare engineering*, vol. 2018, 2018.
- [10] H. Hellbrück, G. Ardel, P. Wegerich, and H. Gehring, "Brachialis Pulse Wave Measurements with Ultra-Wide Band and Continuous Wave Radar, Photoplethysmography and Ultrasonic Doppler Sensors," *Sensors*, vol. 21, no. 1, 2021.
- [11] S. Brovoll, T. Berger, Y. Paichard, Ø. Aardal, T. S. Lande, and S.-E. Hamran, "Time-lapse imaging of human heartbeats using UWB radar," in *IEEE Biomedical Circuits and Systems Conference (BioCAS)*, 2013, pp. 142-145: IEEE.
- [12] L. Ren, Y. S. Koo, H. Wang, Y. Wang, Q. Liu, and A. E. Fathy, "Noncontact multiple heartbeats detection and subject localization using UWB impulse Doppler radar," *IEEE Microwave and Wireless Components Letters*, vol. 25, no. 10, pp. 690-692, 2015.
- [13] T. T. Vo, M. McGuinness, A. F. Hegarty, S. B. O'Brien, K. O'Sullivan, and S. Healy, "Detecting heart rate while jogging: blind source separation of gait and heartbeat," *J Mathematics-in-Industry Case Studies*, vol. 7, no. 1, pp. 1-12, 2017.
- [14] Y. Xu, S. Dai, S. Wu, J. Chen, G. Fang, and R. Sensing, "Vital sign detection method based on multiple higher order cumulant for ultrawideband radar," *IEEE Transactions on Geoscience*, vol. 50, no. 4, pp. 1254-1265, 2011.
- [15] V. Nguyen, A. Q. Javaid, and M. A. Weitnauer, "Harmonic Path (HAPA) algorithm for non-contact vital signs monitoring with IR-UWB radar," in *IEEE Biomedical Circuits and Systems Conference (BioCAS)*, 2013, pp. 146-149: IEEE.
- [16] V. Nguyen, A. Q. Javaid, and M. A. Weitnauer, "Spectrum-averaged Harmonic Path (SHAPA) algorithm for non-contact vital sign monitoring with ultra-wideband (UWB) radar," in *36th Annual International Conference of the IEEE Engineering in Medicine and Biology Society*, 2014, pp. 2241-2244: IEEE.
- [17] S. Kuklin, A. Dzizinskii, Y. M. Titov, and A. Temnikov, "Continuous wavelet analysis: a new method for studying nonstationary oscillations in the cardiac rhythm," *Human Physiology*, vol. 32, no. 1, pp. 116-121, 2006.
- [18] M. V. Prakasam and P. H. Vardini, "Analysis and Applications of Continuous Wavelet Transform," *Suraj Punj Journal For Multidisciplinary Research*, vol. 9, no. 4, pp. 192-195, 2019.
- [19] G. A. Johnson, "Means and method for subtracting dc noise from electrocardiographic signals," ed: U.S. Patent 3580243A, May. 25, 1971.
- [20] M. Le, "Heartbeat extraction based on a high order derivative for ultra-wideband impulse radar application," *Journal of Physics D: Applied Physics*, vol. 53, no. 18, p. 18LT02, 2020.
- [21] M. Le and B. Van Nguyen, "Multivariate Correlation of Higher Harmonics for Heart Rate Remote Measurement using UWB Impulse Radar," *IEEE Sensors Journal*, vol. 20, no. 4, pp. 1859-1866, 2019.
- [22] M. Le, "Heart rate extraction based on eigenvalues using UWB impulse radar remote sensing," *Sensors and Actuators A: Physical*, vol. 303, p. 111689, 2020.
- [23] M. Yochum, C. Renaud, and S. Jacquir, "Automatic detection of P, QRS and T patterns in 12 leads ECG signal based on CWT," *Biomedical Signal Processing and Control*, vol. 25, pp. 46-52, 2016.
- [24] F. Mahmood, M. Toots, L.-G. Öfverstedt, and U. Skoglund, "Algorithm and Architecture Optimization for 2D Discrete Fourier Transforms with Simultaneous Edge Artifact Removal," *International Journal of Reconfigurable Computing*, vol. 2018, p. 1403181, 2018/08/06 2018.
- [25] H.-C. Lin, Y.-C. Ye, B.-J. Huang, and J.-L. Su, "Bearing vibration detection and analysis using enhanced fast Fourier transform algorithm," *Advances in Mechanical Engineering*, vol. 8, no. 10, p. 1687814016675080, 2016/10/01 2016.
- [26] S. Biskri, J.-P. Antoine, B. Inhester, and F. Mekideche, "Extraction of solar coronal magnetic loops with the directional 2D morlet wavelet transform," *Solar Physics*, vol. 262, no. 2, pp. 373-385, 2010.
- [27] C. Chen and X. Chu, "Two-dimensional Morlet wavelet transform and its application to wave recognition methodology of automatically extracting two-dimensional wave packets from lidar observations in Antarctica," *Journal of Atmospheric and Solar-Terrestrial Physics*, vol. 162, pp. 28-47, 2017.
- [28] Y. Rong, *Practical environmental statistics and data analysis*. ILM Publications, 2011.
- [29] M. Burguera, R. Gandia, F. J. Chorro, R. GARCÍA-CIVERA, R. Ruiz, and V. LÓPEZ-MERINO, "Continuous heart rate variability monitoring through complex demodulation implemented with the fast Fourier transform and its inverse," *Pacing and Clinical Electrophysiology*, vol. 18, no. 7, pp. 1401-1410, 1995.
- [30] X. Hu and T. Jin, "Short-range vital signs sensing based on EEMD and CWT using IR-UWB radar," *Sensors*, vol. 16, no. 12, p. 2025, 2016.
- [31] J.-P. Antoine, R. Murenzi, P. Vandergheynst, and S. T. Ali, *Two-dimensional wavelets and their relatives*. Cambridge University Press, 2008.
- [32] M. Le, D.-K. Le, and J. Lee, "Multivariate singular spectral analysis for heartbeat extraction in remote sensing of uwb impulse radar," *Sensors and Actuators A: Physical*, vol. 306, p. 111968, 2020.